ASIAN JOURNAL OF PHARMACEUTICAL AND CLINICAL RESEARCH

INNOVARE ACADEMIC SCIENCES
Knowledge to Innovation

Vol 18, Issue 1, 2025

Online - 2455-3891
Print - 0974-2441

Research Article

VIRTUAL SCREENING OF THE ZIMBABWE NATURAL PRODUCTS DATABASE FOR GLUCOKINASE ACTIVATORS

EZEKIEL MAKAMBWA[1], MASTERIA YUNOVILSA PUTRA[2,3,4], ADHA DASTU ILLAHI[5], MUHAMMAD ADIL KHAN[6], ARRY YANUAR[1,2]*

[1]Laboratory of Biomedical Computation and Drug Design, Faculty of Pharmacy, Universitas Indonesia, Depok, Indonesia. [2]National Metabolomics Collaborative Research Centre, Faculty of Pharmacy, Universitas Indonesia, Depok, Indonesia. [3]Research Centre for Vaccine and Drugs, National Research and Innovation Agency (BRIN), Bogor, Indonesia. [4]Faculty of Pharmacy, Universitas Indonesia, Cluster of Health Sciences Building, Depok, West Java, Indonesia, [5]Department of Pharmaceutical Chemistry, Pharmacy, Sekolah Tinggi Ilmu Kesehatan Salsabila Serang, Indonesia, [6]Department of Clinical Pharmacy, Faculty of Pharmacy, Universitas Indonesia, Depok, West Jawa-16424, Indonesia.

***Corresponding author: Arry Yanuar; Email: arry.yanuar@ui.ac.id**

Received: 03 November 2024, Revised and Accepted: 20 December 2024

ABSTRACT

Objective: This study aimed to identify potential glucokinase activators from Zimbabwean natural products using virtual screening techniques.

Methods: Twenty-one compounds filtered from ChEMBL ID 3820 (pEC50 ≥ 8) were used to generate a pharmacophore model, validated with DUD-E data. This model was employed to screen the 6,220 compounds in the Zimbabwe Natural Products Database (ZiNaPoD) using LigandScout. Hit compounds were docked with glucokinase (protein ID 4NO7) using AutoDock Vina and AutoDock 4 in PyRx, followed by adsorption, distribution, metabolism, and excretion (ADME) screening by SwissADME. Molecular dynamics simulations were conducted on the resulting complexes using the CHARMM36m force field on GROMACS.

Results: The validated pharmacophore model (80% accuracy, 95% sensitivity, 80% specificity) produced 149 hits, 16 of which had binding energies ≤ −8 kcal/mol after the two rounds of molecular docking. The ADME analysis narrowed the selection to four compounds, with binding energies ranging from −8.35 to −9.82 kcal/mol. All four demonstrated stability in molecular dynamic simulations, with average root mean square deviation (RMSD) values ranging from 1.491 to 3.835 Å. The Sphenostylisin I and Dihydroxymethyl dihydroxybenzyl chromanone (DMDBC) complexes exhibited the highest stability with average RMSD values of 1.491±2.794 Å and 2.875±1.452 Å, respectively. They also exhibited low-binding free energies of −30.30±0.38 and −30.20±0.49 kcal/mol, making them promising targets.

Conclusion: Four potential glucokinase activators were identified, with Sphenostylisin I and DMDBC showing promise as candidates for developing new diabetes treatments due to their stability, favorable binding, and absence of liver-toxic groups.

Keywords: Diabetes mellitus, Glucokinase, Molecular docking, Molecular dynamics, Natural products, Pharmacophore modeling, Virtual screening, Zimbabwe.

 DOI: http://dx.doi.org/10.22159/ajpcr.2025v18i1.53258. Journal homepage: https://innovareacademics.in/journals/index.php/ajpcr

INTRODUCTION

The global prevalence of diabetes has seen a significant increase over the past two decades and is projected to exceed 12.5% by 2030, highlighting a growing health challenge worldwide [1]. Type 2 Diabetes Mellitus (T2DM), which is the insensitivity of insulin receptors (pancreatic beta cells) leading to hyperglycemia, accounts for 90% of all diabetes cases [2]. Due to the high cost, general lack of conventional medication, and lifestyle, a lot of people, especially in low-income countries, use medicinal plants to achieve glycemic control [3]. This is especially true for numerous Asian and African communities. In Zimbabwe, almost 60% of the recorded 850,000 people living with diabetes were found to achieve glycemic control using herbal medicine [4]. Although this system appears to be effective, most of these medications are administered by traditional healers without consideration for their mechanisms of action, potential side effects, or underlying toxicities. To address these gaps, experimental studies are conducted to evaluate the effects of the molecules under investigation on the therapeutic target.

Numerous studies have identified multiple therapeutic targets for managing T2DM, each with distinct mechanisms of action, side effects, and other properties [2]. This led to the discovery of classes of drugs associated with certain therapeutic targets, with some classes being explored more than others due to seemingly positive results. These established classes include Sulfonylureas (SU), SGLT (Sodium-Glucose Cotransporter Type 2 inhibitors), GLP1R (Glucagon-like Peptide-1 Receptor agonists) and DPP4 (dipeptidyl peptidase-4 inhibitors). These and other classes are responsible for over 66 diabetes drugs currently circulating [2]. Despite all these, only 30–50% of people with diabetes achieve glycemic control i.e. glycated hemoglobin (HbA1c) <7.0% (<53 mmol/mol) [5]. This is due to different factors including; struggle by patients to adhere to medication, lifestyle factors, socioeconomic factors like lack of access to adequate medication, comorbidities like hypertension leading to adverse effects of drug–drug interactions, and a general individual variability to treatment influenced by genetic factors [5,6]. This means that the search for better drugs remains ongoing, and one of the best methods for discovering new drugs is by either discovering new targets or exploring underexplored targets. One of these promising targets is Glucokinase (GK), also known as Hexokinase IV or Hexokinase D [2,7–9]. GK is mainly expressed in the cells of the pancreas and liver in the human body [10].

In pancreatic beta cells, its primary job is to regulate insulin release based on glucose levels by phosphorylating glucose and using glucose metabolism to create a significant amount of adenosine triphosphate (ATP) as blood glucose levels rise [8]. Furthermore, it deactivates the potassium ATP channels on the islet cell surface, as a result, when Ca^{2+}

influx occurs, the islet cells release insulin, which lowers the blood glucose content [8]. It can exist in 3 states; closed state, open state, and super-open state. However, only the first two states are responsible for its glucose regulatory activities [8]. A glucokinase activator (GKA) is a molecule that can bind to an allosteric site of GK and keep it from going to the third state [8].

In liver cells, lowering of blood glucose levels is the result of the GK enzyme converting glucose to Glucose-6-Phopsphate (G-6-P), which in turn causes glucose to be absorbed, stored as glycogen, and inhibited in liver hepatocytes during the process of gluconeogenesis (the manufacture of glucose from non-carbohydrate sources) [9]. GK regulating proteins (GKRP) can competitively bind GK with glucose, prevent GK from catalyzing the process of glucose phosphorylation to G-6-P, and regulate GK activity in liver cells [8]. Small molecules that connect allosterically to the GK enzyme or interfere with the GK-GKRP complex can work as GKAs [9].

GK activity was discovered in the 1990s and it gained the attention of numerous scientists, leading to a lot of study into GKAs [7]. This eventually led to clinical trials of several GKAs including RO028167, AMG 151 and Piragliatin, but none have yet to reach the market due to inappropriate influences on the normal system leading to adverse effects which include hypoglycemia, the start of fatty liver leading to glucolipotoxicity, and hepatic cell lipidosis leading to a high risk of hyperlipidemia [8,9,11]. These adverse effects are predominant in synthetic GKAs and to deal with them, only GKAs with appropriate influence on kinetic parameters of multiple GK targets such as Dorzagliatin and TTP-399 are currently under investigation in Phase-III clinical trials [11,12].

Although most attention is on synthetic GKAs, an interest in plant-derived molecules for GKA development is growing due to the high number of plants known to possess anti-diabetic activity, based on their ethnopharmacological data, but with little experimental data and no clinical data available [13]. This is especially true for the majority African countries, including Zimbabwe, which boasts unique biodiversity and a wealth of traditional medicinal uses [3]. While natural products have been explored as GKAs, few studies focus on biodiversity-rich regions like Zimbabwe. To initiate this drug discovery research, computational methods like virtual repository screening are ideal to inexpensively ascertain the suitability of certain ligands binding with adequate stability to a certain target, as well as to ascertain possible adverse events. The Zimbabwe Natural Products Database (ZiNaPoD) is a diverse repository of therapeutic plants from Zimbabwe, compiled through extensive literature review. Currently under construction, it includes approximately 340 unique plants and 6,220 compounds, selected primarily for their documented traditional medicinal use. This research aims to use the computational methods; pharmacophore modeling, molecular docking, Absorption, Distribution, Metabolism and Excretion (ADME) screening and molecular dynamics simulations; to virtually screen the ZiNaPoD for potential GKAs.

METHODS

Hardware and software

The project was conducted on a Lenovo_Legion T5 26IAB7 12th Gen Intel(R) Core™ i7-12700 with a 2.1GHz CPU, 128GB RAM, and a 64-bit Windows 11 Version 22H2 operating system, though some processes were executed on an HPC using ssh access. KNIME analytics platform (version 5.2.0) was used for the preparation of the small molecules and dataset cleaning. For the pharmacophore modeling and screening, the LigandScout 4.5 build 20230509 [i1_10] software by Inte: Ligand GmbH was used. AutoDockTools (version 1.5.7) was used for the preparation of the protein while AutoDock (version 4.2.6) and AutoDock Vina (version 1.2.0) were used on PyRx (version 1.1) for the molecular docking, and BioVia's Discovery Studio Visualizer (version 24.1.0.23298) was used for the visualization of the molecular interactions along with UCSF ChimeraX (version 1.6.1) and the Protein-Ligand Interaction Profiler (PLIP) (https://plip-tool.biotec.tu-dresden.de/plip-web/plip/) [14,15]. The online tool SwissADME (http://www.swissadme.ch/) was used for ADME property screening, then GROMACS (version 2023) was used along with the CHARMM-GUI interface (https://charmm-gui.org/) for molecular dynamic simulations, then gmx_MMPBSA (Version 1.6.4) was used for binding energy analysis.

Dataset acquisition and preparation

A search of the ChEMBL (https://www.ebi.ac.uk/chembl/) target protein with the id 3820 gave a result of 1378 compounds with recorded half maximal effective concentration (EC_{50}) values. Filtration resulted in a total of 25 compounds with pEC_{50} values higher than or equal to 8 which were then regarded as "active." These molecules were converted to 3D using the RDKit toolkit on KNIME and saved as a single SDF file. They were then used for the generation of pharmacophores, ignoring 4 of the compounds, thus 21 compounds were included in the pharmacophore generation process. For validation, labeled data were downloaded from the DUD-E (https://dude.docking.org/) database as "actives" with 127 compounds and "decoys" with 4798 compounds after 5 decoy duplicates were removed.

Pharmacophore development and screening

Parameters for conformer generation were set such as maximum number of conformations set as 200 and Root Mean Square (RMS) threshold set as 0.8, then all other options were left on default. Ligand-based pharmacophore creation was used with scoring function pharmacophore-ft and atom overlap, pharmacophore type merged feature pharmacophore, number of omitted features were set as 4, maximum number of pharmacophore model set as 10, partially matching features as 1, and the feature tolerance factor was set as 1. iCon Best was used for all database generation for both the validation and library screening. After an optimum pharmacophore model was generated, 6220 compounds were then loaded from the ZiNaPoD database as the screening library. Virtual screening mode was performed using scoring function pharmacophore-ft with screening mode "match all query features", retrieval mode "get best matching conformation", and maximum number of omitted features was set to 0.

Validation of pharmacophore

The validation phase consisted of screening 2 libraries, one of known actives and another of recorded decoys from DUD-E. After screening, the Receiver Operating Characteristic (ROC) curve was plotted between the percentage retrieved actives (sensitivity) and percentage retrieved decoys (1-specificity). It came along with the Area Under Curve (AUC) at different percentages of the library screening, the Enhancement Factor (EF) at different percentages of the library screening, true positives (TP), and false positives (FP). True negatives (TN) and false negatives (FN) were calculated using the formulae $TN = actives - TP$, and $FN = decoys - FP$. The performance metrics: Sensitivity (SE), Specificity (SP), and Accuracy (AC) were calculated using the formulae $SE = TP/(TP + FN)$, $SP = TN/(TN + FP)$, and $AC = TP + TN/(Total\ compounds)$ [12].

Molecular docking

The protein structure with a PDB id of 4NO7, a resolution of 1.70 Å, determined using X-Ray diffraction, was selected as the target protein and retrieved from the Protein Data Bank (https://www.rcsb.org/) as a PDB file. This crystal structure was selected for different reasons, including that it is recorded in the active conformation of human glucokinase and is activated by a ligand named 2N8, which is recorded as Piragliatin on PubChem [16]. The online tool P2Rank is a fast, stand-alone, template-free tool that uses machine learning to predict ligand binding sites with superior accuracy compared to widely used tools [17]. Along with BioVia's discovery studio, P2Rank was used to select the allosteric site (Fig. 1).

The crystal structure was loaded into AutoDockTools where water molecules were removed, polar hydrogens were added and Kolmann charges were computed, then it was saved as a pdbqt file and later loaded to the PyRx application. Piragliatin was added, as a control, to the

hits of pharmacophore modeling, then they were loaded to the KNIME analytics platform where they were converted from SMILES to 3d molecules, had Hydrogens added, and had their geometries optimized, then they were saved as a single SDF file which was later loaded to PyRx. The mmff94 energy field was used to minimize the loaded ligands which were then converted to the AutoDock format and loaded onto the screening platform. The grid box was set as Grid center X: −9.108; Y: 3.147; Z: 20.313, number of points X: 40; Y: 40, Z: 40, and a spacing of 0.375 in accordance with the number 1 active site according to P2Rank, BioVia's Discovery Studio as well as previous studies [8,16,18]

An exhaustiveness of 120 was used with 200 modes created for the first docking round using the simplified scoring function on AutoDock Vina [19], with all other options left on default. Using the semi-empirical free energy scoring function on AutoDock 4 [20], the Genetic Algorithm was then used with 50 runs, 150 individuals in population, 2 500 000 maximum number of energy evaluations, an rmsd-tolerance of 2.0 A, and all other options were left on default. The standard criterion for docking validation is determining the RMSD between the docked and crystallographic ligand positions, with success defined as an RMSD below 2 Å [21,22]. The native ligand was redocked for validation which was analyzed using Biovia's Discovery Studio and DockRMSD. DockRMSD is useful for docking validation because it provides symmetry-corrected RMSD calculations by identifying the optimal atomic correspondence between the reference and docked ligands, ensuring accurate pose evaluation even for molecules with symmetrical or interchangeable atoms [23].

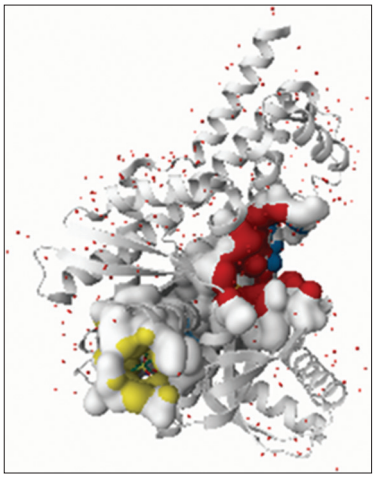

Fig. 1: Highest ranked predicted binding sites of PDB 4NO7, the allosteric site is shown in yellow while the orthosteric (active) site is shown in red

ADME screening

Molecules with binding energies < −8.00 kcal/mol were loaded to the online tool SwissADME where the following parameters were assessed: Pharmacokinetics, Drug-Likeness Filters, Safety and Toxicity, Bioavailability, Water Solubility, and Lipophilicity (Table 1) [24].

Molecular dynamics

Molecular dynamic (MD) simulations were performed using GROMACS to investigate the structural and dynamic properties of the system [30]. The CHARMM36m force field was utilized to generate the topology and parameter files through the CHARMM-GUI interface. The system was solvated in a rectangular simulation box filled with TIP3P water molecules, and ion placement was conducted using the Monte Carlo method to neutralize the system and achieve a physiological NaCl concentration of 0.15 M. The pH of the system was set to 7.4 to simulate near-physiological conditions [31,32].

Energy minimization was conducted using the steepest descent algorithm to remove steric clashes and optimize system stability. The system was subsequently equilibrated for 100 ps. Temperature control was maintained at 310 K through the V-rescale thermostat, while the pressure was regulated at 1 bar using the C-rescale barostat. The production phase of the simulation was performed for 100 ns under the NPT ensemble, with a time step of 2 fs. Bond constraints involving hydrogen atoms were applied using the LINCS algorithm to ensure accurate integration of motion. Long-range electrostatic interactions were calculated using the Particle Mesh Ewald (PME) method, with a 1.2 nm cutoff for both electrostatic and Van der Waals interactions. Simulation trajectories were saved every 10 ps for subsequent analyses.

Table 1: ADME screening rationale used for docking results, including categories, parameters, brief descriptions, and selection criteria (in brackets)

Category	Parameter	Description
Pharmacokinetics (Any molecule that tested positive in at least 3/6 of the given parameters was considered for subsequent analysis)	Gastrointestinal (GI) absorption	The process by which a drug or substance is absorbed from the gastrointestinal tract into systemic circulation is critical to its bioavailability. A higher GI absorption indicates greater systemic absorption of the drug [25]. (High GI absorption was desired)
	P-glycoprotein substrate (Substrates were desired)	Among other effects, they lead to the increase in the GI absorption power of drugs [26].
	CYP 450 inhibition: CYP2C19, CYP2C9, CYP2D6, CYP3A4	Inhibition of any of the enzymes can cause disruptions like drug–drug interactions that can lead to adverse events [27]. (Non-inhibitors were counted)
Drug-Likeness	Filters: Lipinsiki, Ghose, Veber, Egan.	These are set rules to determine whether a molecule has the capacity to be developed into a drug.
	Bioavailability	Bioavailability Score
Safety and Toxicity	PAINS (Pan Assay Interference Compounds)	They usually indicate high chances of false positives when detected.
	Brenk	These are small fragments of a molecule that could be toxic, chemically reactive, metabolically unstable, etc.,
Water solubility	(Log S (ESOL), Log S (Ali), and Log S (SILICOS-IT)	This is an average of the named solubilities. Better solubility enhances drug absorption into the bloodstream, improving delivery to the site of action [28]. (Only molecules that were considered moderately soluble or better were included)
Lipophilicity	Consensus Log Po/w	This is calculated from various lipophilicity parameters. A lipophilicity range of 1–3 strikes a balance between good solubility, permeability, and binding affinity, while minimizing potential toxicity [29].

Post-simulation analyses included the calculation of Root Mean Square Deviation (RMSD) to evaluate overall structural stability, Root Mean Square Fluctuation (RMSF) to assess the flexibility of individual residues throughout the simulation, and Molecular Mechanics Poisson-Boltzmann Surface Area/Generalized Born Surface Area (MM-PBSA/MM-GBSA) for the binding free energy from the complex between ligand and protein. The graphical plots were viewed using xmgrace while the MM-PBSA/MM-GBSA analyses were performed using gmx_MMPBSA on a Conda environment [33,34]. Analyses were done for entirety of the simulation process.

RESULTS AND DISCUSSION

Pharmacophore modeling

The pharmacophore model validation involved selecting a model that balanced the chosen validation parameters to optimize selection while minimizing the exclusion of true positives. This balance was achieved with model 6, as highlighted in Table 2.

Model 6 (Fig. 2) was selected for screening the library, yielding a hit rate of 2.4%, corresponding to 149 hits out of 6,220 compounds in the ZiNaPoD database. Fig. 2a illustrates the pharmacophoric features of the model, which include two hydrogen bond acceptors, two aromatic rings, one hydrogen bond donor, and one hydrophobic group. Validation results demonstrated that model 6 is 80% accurate, 80% specific, and 95% sensitive, offering optimal selectivity, as evidenced by the Receiver Operating Characteristics (ROC) curve in Fig. 2b.

Molecular docking

Docking validation involves assessing the docking protocol using methods appropriate to the available structural data. Since this simulation utilized the same binding site as the native ligand, re-docking was deemed the most suitable validation approach. The re-docking process was performed using DockRMSD, resulting in an RMSD of 0.8280 Å (Fig. 3).

To achieve more refined results, two rounds of molecular docking were conducted. The first round, performed using AutoDock Vina, identified 40 compounds with binding energies below −8 kcal/mol. These compounds were further screened using AutoDock 4, resulting in 17 compounds (including the reference compound Piragliatin) with binding energies below −8 kcal/mol, as listed in Table 3. The reference compound Piragliatin exhibited the lowest binding energy (−12.41 kcal/mol), followed by Robinetinidol 3-O-gallate (−10.64 kcal/mol), Prostratol C (−10.44 kcal/mol), and Nitidulan (−10.19 kcal/mol). The remaining molecules showed binding energies ranging from −8.19 to −9.98 kcal/mol. These 17 compounds were subsequently subjected to ADME analysis, based on the criteria outlined in Table 1, leading to the selection of four compounds for further investigation.

The selected compounds exhibited ADME properties comparable to Piragliatin, with Atranorin showing the least favorable profile due to broken Brenk rules and its inability to act as a glycoprotein substrate, leading to higher toxicity potential. Similarly, Camptothecin also could not act as a glycoprotein substrate, though it adhered to all Brenk rules. In contrast, Dihydroxymethyl dihydroxybenzyl chromanone (DMDBC) demonstrated an ADME profile similar to Piragliatin, while Sphenostylisin I showed a superior profile by avoiding interactions with three out of four CYP450 proteins, reducing the likelihood of system disruption. Although the top-ranking compounds showed higher binding energies compared to the reference compound Piragliatin, they demonstrated relatively low-binding energies: Atranorin (−8.35 kcal/mol), Camptothecin (−9.82 kcal/mol), DMDBC (−8.53 kcal/mol), and Sphenostylisin I (−8.9 kcal/mol). In a study by Khamlich on the screening of Chinese traditional medicinal plant compounds for glucokinase activators, molecular docking yielded binding affinities ranging from −6.7 to −8.6 kcal/mol for Swertiamarin, Apigenin, Mangiferin, and Tatanan A [35]. Notably, Mangiferin, with a binding affinity of −7.7 kcal/mol, had already been validated as a potential GKA through in vitro and in vivo studies [36]. These comparisons suggest a strong potential

Table 2: Generated pharmacophore models validated using various metrics; the selected model is highlighted in yellow

Model	$AUC_{100\%}$[1]	$EF_{1\%}$[2]	Sensitivity	Specificity	Accuracy	Pharmacophore	Exclusion Vols
1	0.9	26.1	0.827	0.933	0.931	H[3], A[4], A, HBA[5], HBD[6]	22
2	0.9	26.9	0.827	0.935	0.932	H, A, A, HBA, HBD	22
3	0.89	28.5	0.803	0.933	0.93	H, A, A, HBA, HBD	23
4	0.91	27.7	0.835	0.931	0.929	H, A, A, HBA, HBD	22
5	0.86	30.9	0.732	0.957	0.952	H, A, A, HBA, HBA, HBD	32
6	0.94	24.5	0.953	0.799	0.803	H, A, A, HBA, HBA, HBD	32
7	0.91	22.2	0.913	0.792	0.796	H, A, A, HBA, HBA, HBD	31
8	0.92	19	0.961	0.782	0.786	A, A, HBA, HBA, HBD	25
9	0.95	27.7	1	0.639	0.649	A, A, HBA, HBA, HBD	25
10	0.94	27.7	1	0.631	0.64	A, A, HBA, HBA, HBD	23

[1]Area under the curve at 100% of the screening, [2]Enrichment factor at 1%, [3]Hydrophobic, [4]Aromatic, [5]Hydrogen bond acceptor, [6]Hydrogen bond donor

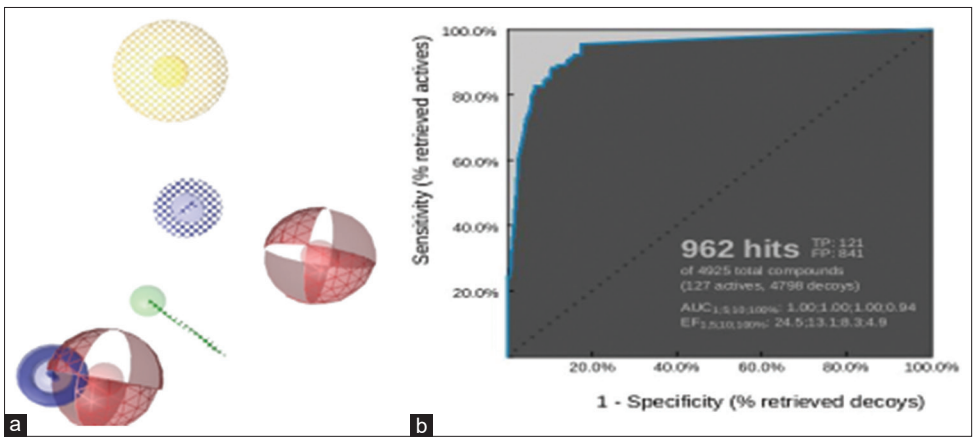

Fig. 2: (a) Pharmacophoric features of the selected pharmacophore model, model 6, excluding exclusion volumes. (b) ROC plot of the selected pharmacophore model

for the selected compounds to function as GKAs. However, it is worth noting that, while Piragliatin also demonstrated promising results in preclinical trials and passed a double-blind, placebo-controlled, multiple-ascending-dose safety study in patients with type 2 diabetes mellitus [37], it ultimately failed in phase 2 clinical trials due to liver toxicity associated with long-term use. This toxicity arises from the metabolization of its cyclopentanone group into an alcohol in the liver [8]. As shown in Fig. 4, the oxygen of the cyclopentanone group lacks significant interaction with the protein, making it more prone to metabolic conversion into a toxic alcohol.

Despite slightly higher binding energies compared to Piragliatin, Sphenostylisin I and DMDBC formed extensive hydrophobic and hydrogen-bonding interactions, particularly with key residues such as ARG 63, TYR 214, and GLU 67, which likely contributed to their stability.

Atranorin and Camptothecin, while showing comparable or better binding energies, lacked robust π-π stacking or formed fewer stabilizing interactions, limiting their potential as glucokinase activators. These results suggest that Sphenostylisin I and DMDBC balance binding affinity and interaction profile, making them promising candidates for further investigation. A detailed examination of each compound also highlighted additional expected results, providing insights into their potential activity.

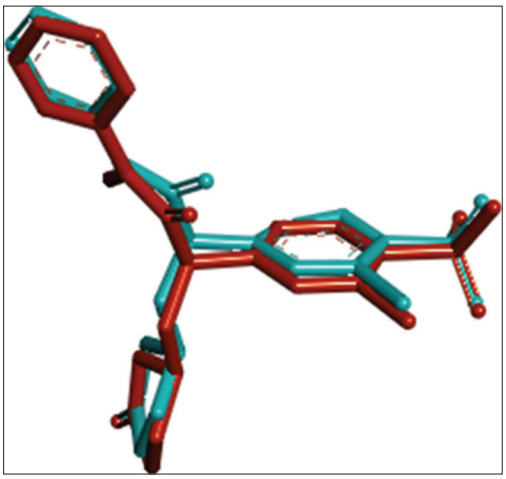

Fig. 3: Docking validation. The docked ligand (red), compared to the native ligand (blue) using BioVia discovery studio

Atranorin is a depside containing aromatic rings, ester linkages, and an aryl aldehyde group (Fig. 5). While aldehydes are typically reactive, the aryl aldehyde group in Atranorin is expected to metabolize into safer byproducts, reducing the risk of liver damage [38]. In a study by Melo *et al*., Atranorin was shown to be non-cytotoxic and exhibited redox properties that provided cytoprotective effects, safeguarding SH-SY5Y cells from H_2O_2-induced oxidative stress and viability loss [39]. These redox properties enhance Atranorin's potential as a dual-action GKA, improving glucokinase activity while protecting pancreatic cells from oxidative stress. This dual functionality makes it a strong candidate for further investigation. As shown in Table 4, the interaction profile of the Atranorin-Glucokinase complex is comparable to that of Piragliatin-Glucokinase, particularly in the distribution of interaction types. Notably, the Atranorin-Glucokinase complex exhibits a higher number of hydrogen bonds than Piragliatin-Glucokinase, potentially leading to distinct functional properties, further supporting Atranorin's potential as a GKA.

Camptothecin is a pentacyclic alkaloid (Fig. 6) that can exist in either its lactone or carboxylate form. Despite displaying a favorable ADME profile in this study, it is primarily researched as an anticancer agent due to its ability to target topoisomerase I, leading to DNA damage and apoptosis in cancer cells [40]. However, this mechanism also underpins its toxicity, making it a less suitable candidate as a GKA. Additionally, Camptothecin demonstrated predominantly hydrophobic interactions with GK (Table 4), differing significantly from the reference compound and contributing to its limited therapeutic efficacy [41]. These factors collectively reduce its potential as a viable GKA candidate.

DMDBC (Fig. 7) is a chromanone, an oxygen-containing heterocyclic compound. While limited information is available on this specific molecule, other chromanones have demonstrated various therapeutic properties with low toxicity [41,42]. This highlights a gap in the literature, warranting further analysis of DMDBC. Notably, its binding interactions with GK (Table 4) are well-distributed, even exceeding those of Atranorin, which reinforces its potential as a GKA.

Sphenostylisin I is a carbonyl compound featuring a benzofuran and a phenyl sidechain (Fig. 8). Although limited data exists on its specific behavior, its individual components provide some insight into potential toxicity. The carbonyl group increases susceptibility to reduction and conjugation reactions in the liver, potentially forming various metabolites. This is similar to the metabolic pathways observed in Spirotetramat analogs, where specific functional groups influenced

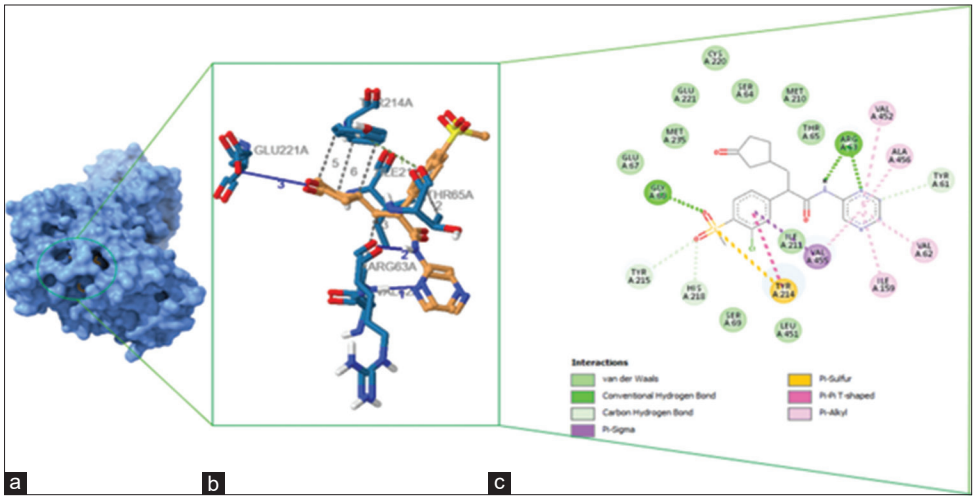

Fig. 4: Piragliatin-Glucokinase complex, (a) the surface view of the ligand (orange) docked inside the protein (blue), (b) 3D view of the interactions of the ligand (orange) with the close ammino residues (blue), (c) 2D view of the interactions of the central ligand with surrounding ammino acid residues Despite Piragliatin's toxicity, its interaction with the allosteric site of GK activates the enzyme. This interaction was evaluated for the top-ranking compounds (Table 4)

Table 3: Top 17 AutoDock molecular docking hits filtered by SWISSADME[1]. Top-ranked compounds are highlighted in yellow while the reference compound Piragliatin

Ligand	Binding Energy (kcal/mol)	Pharmacokinetic			Drug likeness				Safety and Toxicity		Bioavailability (>=0.55)	Solubility (>=moderate)	Lipophilicity (1–3)
		CPY450[2]	GI Absorption	P-glycoprotein	Lipinsiki	Veber	Ghose	Egan	PAINS[3]	Brenk			
Piragliatin	−12.41	2	✓	✓	✓	✓	✓	✓	✓	✓	✓	✓	✓
Atranorin	−8.35	4	✓	✗	✓	✓	✓	✓	✓	2	✓	✓	✓
Bolusanthol B	−9.52	1	✓	✗	✓	✓	✓	✓	1	2	✓	✓	✓
Camptothecin	−9.82	3	✓	✗	✓	✓	✓	✓	✓	✓	✓	✓	✓
Catechin gallate	−8.76	4	✗	✗	1	1	✓	1	1	2	✓	✓	✓
DMDBC	−8.53	2	✓	✗	✓	✓	✓	✓	✓	✓	✓	✓	✓
Erythribyssin E	−9.98	0	✓	✓	✓	✓	✓	✓	✓	1	✓	✓	✗
(3S)-6,7-dimethoxy-3-[2-(2-methoxyphenyl)-2-oxoethyl]-3H-2-benzofuran-1-one	−8.36	0	✓	✗	✓	✓	✓	✓	✓	✓	✓	✓	✓
7-hydroxy-2-methyl-6-[β-galactopyranosyl-propyl]-4H-chromen-4-one	−8.19	4	✗	✗	✓	1	✓	1	✓	✓	✓	✓	✗
Licoisoflavone A	−9.49	2	✓	✓	✓	✓	✓	✓	✓	1	✓	✓	✗
Nitidulan	−10.19	0	✓	✗	✓	✓	1	✓	✓	1	✓	✗	✗
Pectachol	−9.18	2	✓	✓	✓	✓	✓	✓	✓	2	✓	✗	✗
Prostratol C	−10.44	0	✓	✗	✓	✓	✓	✓	✓	1	✓	✓	✗
Robinetinidol 3-O-gallate	−10.64	4	✗	✗	1	1	✓	1	1	1	✓	✓	✓
Sativan	−8.38	1	✓	✗	✓	✓	✓	✓	✓	✓	✓	✓	✓
Sphenostylisin I	−8.9	3	✓	✓	✓	✓	✓	✓	✓	✓	✓	✓	✓
Sphenostylisin K	−8.84	1	✓	✗	✓	✓	✓	✓	✓	1	✓	✓	✓

[1]The tick represents a pass, while the X represents a failure. The CPY450 numbers represent the number of passes (non-inhibitors) recorded for the 4 proteins, and the other numbers represent the number of rules broken,
[2]Cytochrome P450 proteins CYP2C19, CYP2C9, CYP2D6, CYP3A4, [3]Pan-Assay Interference Compounds

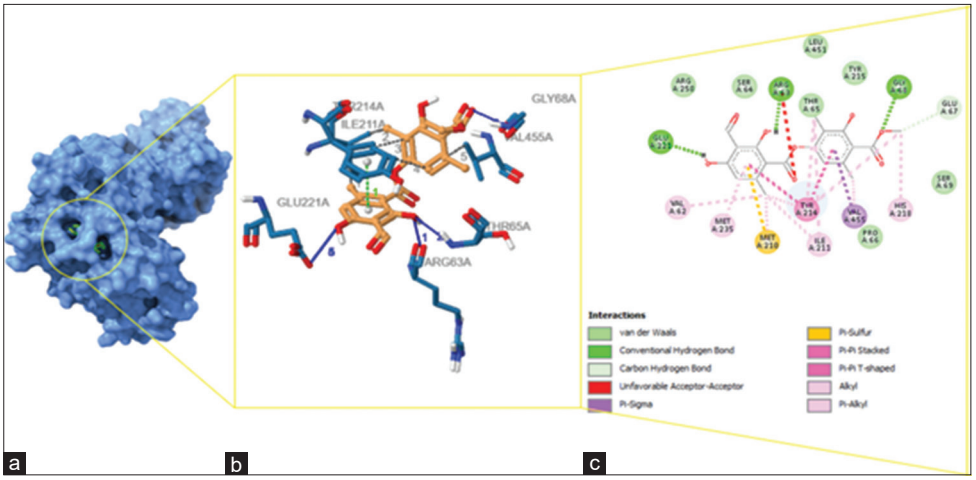

Fig. 5: Atranorin-Glucokinase complex, (a) the surface view of the ligand (orange) docked inside the protein (blue), (b) 3D view of the interactions of the ligand (orange) with the close ammino residues (blue), (c) 2D view of the interactions of the ligand (orange) with surrounding ammino acid residues

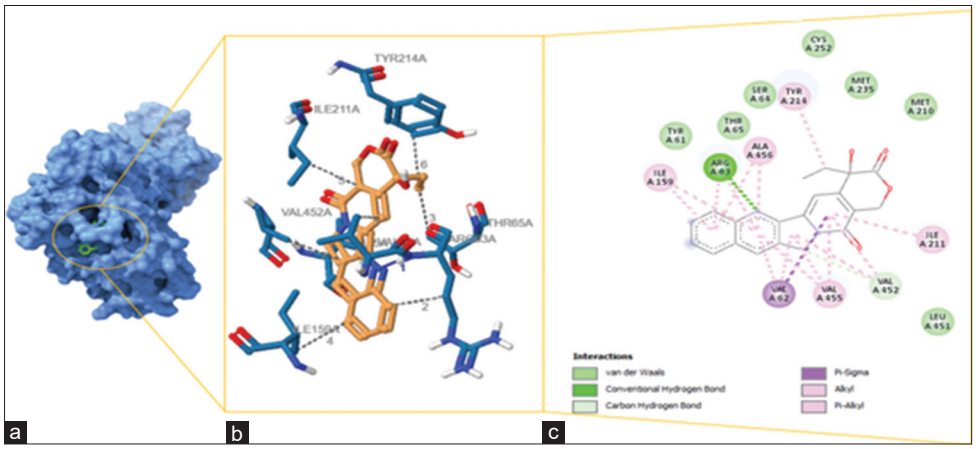

Fig. 6: Camptothecin-Glucokinase complex, (a) the surface view of the ligand (orange) docked inside the protein (blue), (b) 3D view of the interactions of the ligand (orange) with the close ammino residues (blue), (c) 2D view of the interactions of the central ligand with surrounding ammino acid residues

Table 4: Interactions of Ligands with Glucokinase

Ligand	Interaction type	Residue (Distance, Angstrom)
Piragliatin	Hydrophobic	VAL 62 (3.58); THR 65 (3.58); ILE 211 (3.55); ILE 211 (3.87); TYR 214 (3.26); TYR 214 (3.77); TYR 214 (3.74)
	Hydrogen donor	ARG 63 (1.84); GLU 221 (3.35)
	Hydrogen Acceptor	ARG 63 (2.15)
	Pi-Pi Stacking	TYR 214 (4.47)
Atranorin	Hydrophobic	ILE 211 (3.06); ILE 211 (3.07); TYR 214 (3.17); TYR 214 (3.59); VAL 455 (3.85)
	Hydrogen donor	THR 65 (2.28); GLY 68 (1.84); GLU 221 (2.87)
	Hydrogen Acceptor	ARG 63 (2.18); GLU 221 (2.84)
	Pi-Pi Stacking	TYR 214 (3.60)
Camptothecin	Hydrophobic	VAL 62 (3.01); ARG 63 (3.64); THR 65 (3.56); ILE 159 (3.96); ILE 211 (3.77); TYR 214 (3.76); VAL 452 (3.45); VAL 455 (3.47)
	Hydrogen donor	ARG 63 (1.86)
DMDBC	Hydrophobic	VAL 62 (3.19); GLU 67 (3.82); ILE 211 (3.23); TYR 214 (3.19); TYR 214 (3.83)
	Hydrogen donor	THR 65 (2.46); GLY 68 (2.16); HIS 218 (3.37)
	Hydrogen Acceptor	ARG 63 (2.05); GLU 67 (2.92); CYS 220 (1.71)
	Pi-Pi Stacking	TYR 214 (4.43)
Sphenostylisin I	Hydrophobic	THR 65 (3.67); ILE 211 (3.59); TYR 214 (3.39); TYR 214 (3.57); TYR 215 (3.31); VAL 455 (2.94)
	Hydrogen donor	THR 65 (1.93); GLU 67 (3.76); GLY 68 (2.57); HIS 218 (3.25)
	Hydrogen Acceptor	ARG 63 (2.70); GLU 67 (3.13); CYS 220 (1.76)
	Pi-Pi Stacking	TYR 214 (3.79); TYR 214 (4.50)

bioactivity and metabolism [43]. However, these moieties are generally expected to yield less severe effects. Related compounds exhibit diverse biological activities, including antioxidant, anti-inflammatory, and anticancer properties, partly due to their metabolic products [44,45].

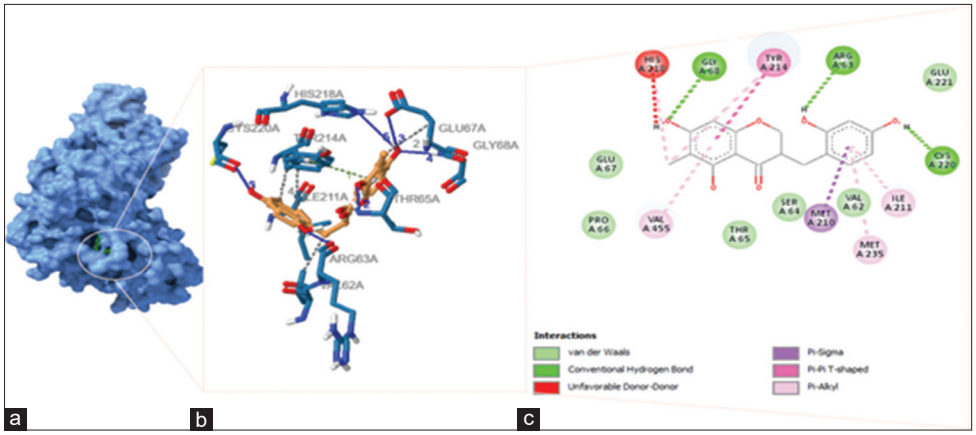

Fig. 7: DMDBC -Glucokinase complex, (a) the surface view of the ligand (orange) docked inside the protein (blue), (b) 3D view of the interactions of the ligand (orange) with the close ammino residues (blue), (c) 2D view of the interactions of the central ligand with surrounding ammino acid residues

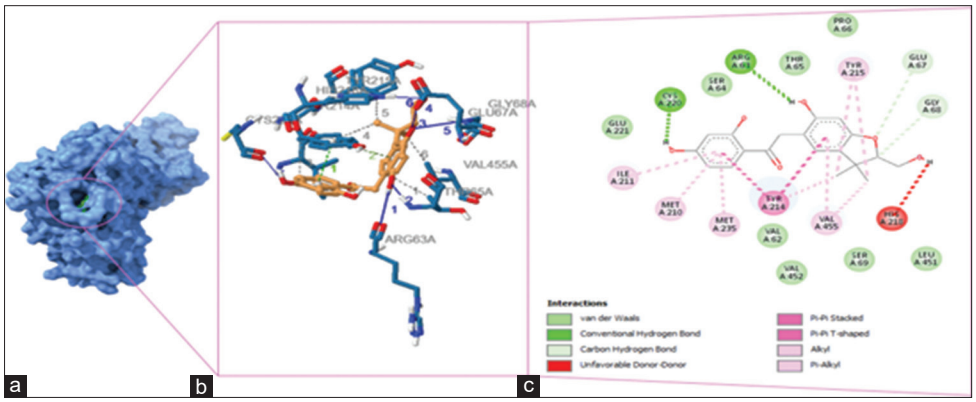

Fig. 8: Sphenostylisin I-Glucokinase complex, (a) the surface view of the ligand (orange) docked inside the protein (blue), (b) 3D view of the interactions of the ligand (orange) with the close ammino residues (blue), (c) 2D view of the interactions of the central ligand with surrounding ammino acid residues

Interaction analysis (Table 4) reveals that Sphenostylisin I forms more hydrogen bonds with GK than Piragliatin, indicating a broader range of interactions that could enhance its potency as a drug.

Molecular dynamics

Molecular dynamic (MD) simulations are performed to evaluate the stability of a system. The outcomes of an MD run can be analyzed through various approaches, including graph plotting, structural visualization, and energy analyses. Following ADME screening, the selected molecular complexes were subjected to MD analysis. In this study, key graphical methods such as RMSD, RMSF, radius of gyration (Rg), and principal component analysis (PCA) were employed. These analyses were complemented by energy evaluations using MMGBSA and MMPBSA. All analyses were conducted over 100 ns simulation runs.

RMSD analysis

The RMSD plot is a key tool in MD analysis, used to assess the stability and conformational changes of protein-ligand complexes throughout the simulation. A stable complex typically exhibits minor fluctuations in RMSD values following the initial equilibration period, signifying that the system has reached a stable conformation. Conversely, significant deviations in RMSD values indicate major structural rearrangements, which can provide valuable insights into the binding mechanism and dynamic behavior of the complex [46].

The ligands, labeled as "UNK," were aligned to the backbone for RMSD analysis, revealing an average RMSD range of 1.491 to 3.835 Å (Fig. 9). Among the ligands, Sphenostylisin I demonstrated the highest stability,

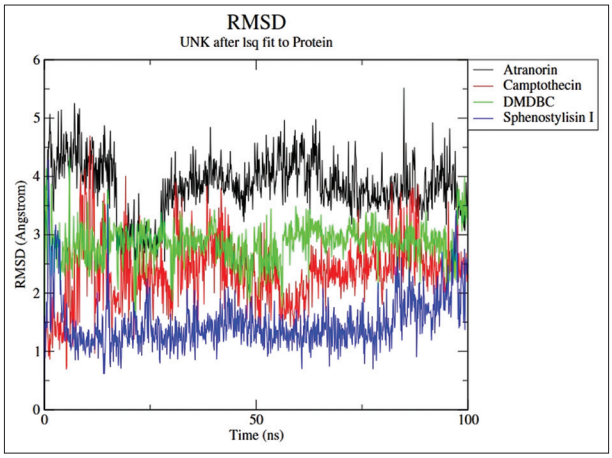

Fig. 9: RMSD plots of the top-ranked ligands' activity during the simulation, highlighting relatively stable systems with notable differences

with the lowest average of 1.491±2.794 Å. The large range is due to the great fluctuations during the initial nanoseconds of the simulation which could be attributed to its unique interactions with the protein, such as the two pi-pi stacking interactions, which may require more time to stabilize. DMDBC also showed high stability, with an average of 2.875±1.452 Å, showing minimal fluctuations throughout the

simulation. Camptothecin displayed an average of 2.357±2.343 Å, showing considerable stability. Atranorin displayed the lowest stability with an average of 3.835±1.684 Å according to RMSD analysis. These findings highlight the potential of Sphenostylisin I and DMDBC as promising GKAs. To further explore localized flexibility and stability, an RMSF analysis was conducted.

RMSF analysis

RMSF is another key metric in protein-ligand MD studies, used to quantify the flexibility of individual amino acid residues. It provides crucial insights into the dynamic behavior of the protein-ligand complex by identifying residues with significant fluctuations, which may play vital roles in ligand binding and protein function [47]. Residues involved in critical interactions, such as hydrogen bonds or hydrophobic contacts, often exhibit lower RMSF values, indicating their contribution to stable interactions. Furthermore, RMSF serves as an indicator of the complex's overall stability, with lower values generally reflecting a more stable system [31].

The RMSF values for all complexes range from approximately 0.8 to 2.2 Å, indicating considerable stability across most residues (Fig. 10). However, slight differences were observed, with Atranorin occasionally exhibiting marginally higher RMSF values, supporting its relatively lower stability as indicated by the RMSD analysis. The Sphenostylisin I complex displayed higher RMSF values at residue 69 (2.849 Å) and residue 458 (2.285 Å), despite these residues not being directly involved in protein-ligand interactions. Interestingly, GLU 67 and GLY 68, located near residue 69, collectively contribute to three hydrogen bonds. The fluctuations at residue 69 reflect the dynamic nature of the local binding environment, suggesting that non-interacting residues can influence or be influenced by nearby interacting residues. These fluctuations may destabilize the hydrogen bonds involving GLU 67 and GLY 68, potentially affecting the stability of the interaction network.

Despite these fluctuations, the Sphenostylisin I complex maintained overall stability, similar to the other complexes, which were also affected in this region. DMDBC consistently exhibited the lowest RMSF values, reinforcing its potential as a strong GKA candidate. To gain further insights into the stability, functionality, and biological relevance of these complexes, compactness was evaluated through the radius of gyration (Rg) analysis, which offers additional context on their dynamic behavior [36].

Radius of gyration analysis

The radius of gyration (Rg) quantifies the compactness of a protein structure by calculating the root mean square distance of the protein's atoms from its center of mass [48]. This metric facilitates comparisons between different molecular states or conditions, offering valuable insights into structural stability and dynamic behavior. Rg is particularly useful in understanding the conformational dynamics of macromolecules, such as revealing the degree of folding or unfolding in proteins, which is an essential aspect when assessing protein stability and interactions [48]. Similar to RMSD and RMSF, larger fluctuations in Rg values indicate reduced stability of the analyzed complexes.

All four systems shown in Fig. 11 exhibited low fluctuations, ranging from 23 to 24.5 Å, indicating general compactness. Sphenostylisin I demonstrated an initial rise from 22.8 Å to around 24 Å within the first 20 ns, after which it stabilized, with fluctuations of less than 0.1 Å around its average value of 24 Å. This suggests overall system stability, supporting its potential as a GKA. DMDBC also maintained considerable stability throughout the simulation, with fluctuations of less than 0.1 Å from its average Rg value of 23.80 Å. Camptothecin showed the highest fluctuation, observed between 40 to 50 ns of the simulation. Atranorin displayed relative compactness, with fluctuations ranging from 23.25 to 24.5 Å. To gain further insights, PCA analysis was performed.

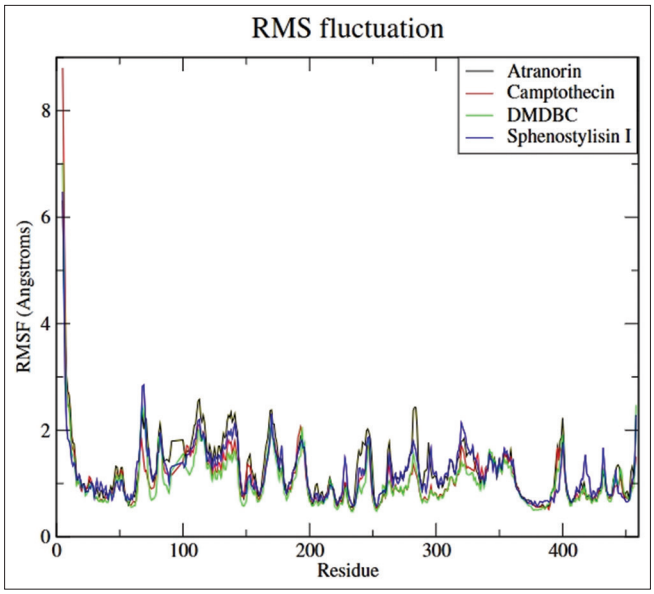

Fig. 10: RMSF plots showing the behavior of the ammino residues in the top-ranked complexes during the simulation, highlighting a common trend of stability

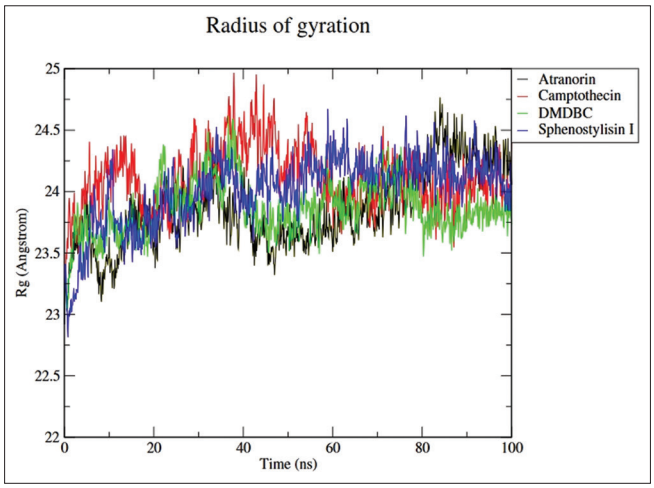

Fig. 11: Rg plots of the top-ranked complexes during the MD run, showing low fluctuations and indicating stability

PCA analysis

Principal Component Analysis (PCA) complements traditional MD analysis by providing a more comprehensive view of molecular motions. It captures essential, collective movements, making it easier to interpret complex data. The principal components (PCs) derived from MD simulations are based on the eigenvectors of the covariance matrix, each reflecting a specific change in the protein's trajectory [49]. A Free Energy Landscape (FEL) or Gibbs Energy Landscape is often used to visualize the system's essential motions or conformations. In this visualization, the x-axis (PC1) and y-axis (PC2) correspond to the first and second principal components, capturing the primary and secondary variances in the dataset, respectively. The blue and green clusters represent the most stable conformational states of the system, where it remains for extended periods. Red regions between clusters indicate energy barriers that the system must overcome to transition between these stable states.

Eigenvectors were first calculated, and the dominant motions were identified by filtering the trajectories to focus on the most relevant movements. The Sphenostylisin I complex exhibits the highest stability, as

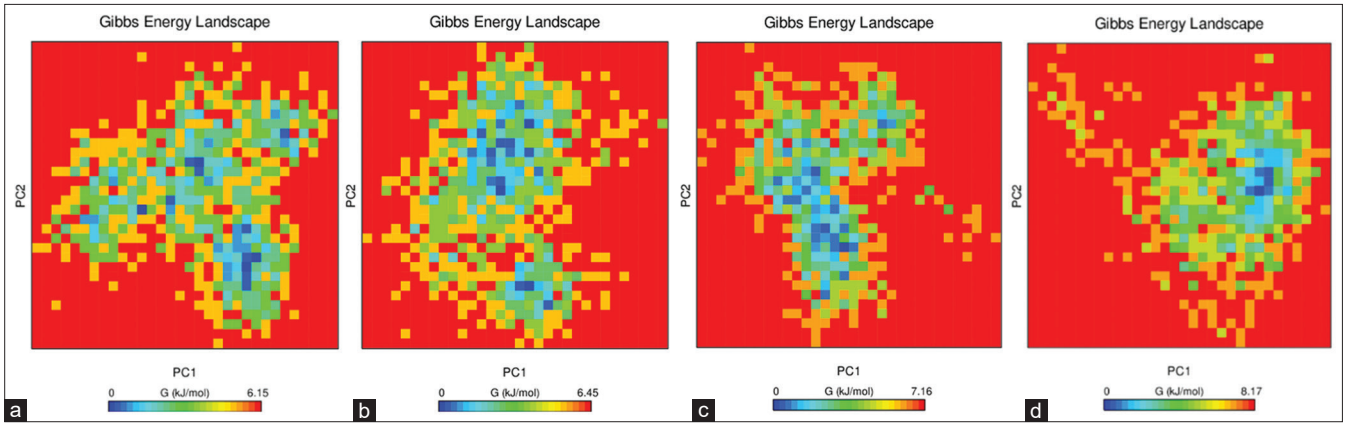

Fig. 12: FEL of the four complexes showing stability differences. Concentrated blue/green indicates higher stability; scattered blue/green suggests lower stability with energy barriers (red). (a) Atranorin, (b) Camptothecin, (c) DMDBC, (d) Sphenostylisin I

Table 5: Average MM-G (P) BSA energies of the protein-ligand complexes with the standard error of the mean (SEM)

Glucokinase Complex	MMGBSA (kcal/mol) Average±SEM	MMPBSA (kcal/mol) Average±SEM
Atranorin	−25.94±0.43	−19.88±0.41
Camptothecin	−28.52±0.38	−22.17±0.38
Dihydroxy	−30.20±0.49	−23.19±0.64
Sphenostylisin I	−30.30±0.38	−23.90±0.56

indicated by its more concentrated cluster, despite some scattered points outside this cluster (Fig. 12d). This suggests that the Sphenostylisin I complex spends most of its time in a single conformation, indicating greater stability. The overall area of the blue/green region for DMDBC (Fig. 12c) is comparable to that of Sphenostylisin I, suggesting stability within a single conformation. However, the DMDBC landscape displays an almost separate region, which suggests some variability in conformations. In contrast, the Atranorin (Fig. 12a) and Camptothecin (Fig 12b) systems show larger regions with several red regions in between, indicating less stable systems. These results further support the potential of Sphenostylisin I and DMDBC as potential glucokinase activators. To further assess the binding stability of the protein-ligand interactions, MM-PBSA/MM-GBSA analyses were performed to estimate the free energy of binding and quantify the stability of the molecular dynamics simulations.

MM-PBSA/MM-GBSA

MMPBSA/MMGBSA methods provide an accurate estimation of binding free energy, offering valuable insights into the strength and stability of protein-ligand interactions. These methods consider solvation effects, including both polar and non-polar contributions, which are crucial for modeling the energetics of the system in a biologically relevant environment [50]. Additionally, MMPBSA/MMGBSA can estimate the entropic contributions to binding, a factor that is often challenging to capture with other computational techniques. By comparing the calculated binding affinities with experimental data, these methods help validate the molecular dynamics simulations, ensuring that the observed interactions are reliable and biologically significant [51].

Since there is no direct method for running MM-GB(PB)SA calculations using GROMACS, a tool developed by Valdes-Tresanco *et al*., was employed. This tool, gmx_MMPBSA, enables complex calculations, including binding free energy and stability assessments. It is accompanied by detailed documentation, including tutorials and test/example files, making it highly accessible for novice users. [34]. The total average binding free energy (ΔG_{bind}) is calculated from the individual energy of the system as follows [34]:

$$\Delta G_{bind} = \langle G_{\text{Complex}} \rangle - \langle G_{\text{Receptor}} \rangle - \langle G_{\text{Ligand}} \rangle$$

Whereas each of these energies is calculated individually $\langle G_x \rangle$ as follows:

$$\langle G_x \rangle = \langle E_{MM} \rangle + \langle G_{sol} \rangle - \langle TS \rangle$$

Where:

$\Delta E_{MM} = \Delta E_{bonded} + \Delta E_{nonbonded} = (\Delta E_{bond} + \Delta E_{angle} + \Delta E_{dihedral}) + (\Delta E_{ele} + \Delta E_{vdW})$

ΔE_{MM} = Molecular mechanical energy changes in the gas phase.

$\langle G_{sol} \rangle$ = Energy of solvation

$\langle TS \rangle$ = Temperature and entropy energy.

MM-GBSA analyses conducted over the entire MD run yielded relatively low-binding energy values, ranging from −25.51 to −30.68 kcal/mol (Table 5). In contrast, MM-PBSA analyses under the same conditions produced higher energy values, ranging from −19.47 to −24.46 kcal/mol. The observed difference of 6–7 kcal/mol between the two methods reflects their distinct approaches to calculating binding free energy. This consistency across methods reinforces the reliability and robustness of the study's findings.

Among the tested compounds, Sphenostylisin I exhibited the highest stability, with binding energies of −30.30 kcal/mol (MM-GBSA) and −23.90 kcal/mol (MM-PBSA), followed closely by DMDBC with values of −30.20 kcal/mol and −23.19 kcal/mol, respectively. These results align with other findings in this research, providing compelling evidence for the potential of Sphenostylisin I and DMDBC as GKAs. Although Atranorin and Camptothecin showed higher binding energies of −19.88 kcal/mol and −22.17 kcal/mol, respectively, their values still suggest reasonable stability, supporting their consideration as moderately stable complexes.

Sphenostylisin I and DMDBC demonstrated exceptional performance across various analyses in this study, underscoring their potential as GKAs. Although their molecular docking binding energies (−8.53 kcal/mol for DMDBC and −8.9 kcal/mol for Sphenostylisin I) were higher than Piragliatin's (−12.41 kcal/mol), their interaction profiles and the findings from literature support their promise as therapeutic candidates. Their stability during MD simulations, favorable ADME properties, and strong binding-free energy values suggest that Sphenostylisin I and DMDBC could behave as effectively as Piragliatin in enhancing glucokinase activity. However, they may present a lower risk of adverse effects, particularly liver toxicity, due to the absence of the cyclopentanone functional group, which was a critical factor in Piragliatin's failure. The lack of such a problematic moiety in Sphenostylisin I and DMDBC indicates a safer pharmacological profile, making them promising candidates for further investigation as glucokinase activators.

The limited research on Sphenostylisin I and DMDBC presents an opportunity for further exploration, as analogous compounds are recognized for multiple therapeutic benefits, including antioxidant

and anti-inflammatory effects [42,43,45,46]. In-depth in vitro and in vivo studies are essential to validate these findings before advancing to optimization and clinical trials. Additionally, exploring other natural product libraries could yield similarly favorable results, aligning with the promising outcomes of this study.

In contrast, Camptothecin and Atranorin exhibited lower stability across most analyses. Camptothecin's known toxicity, stemming from its DNA-damaging properties, significantly reduces its appeal as a GKA. While Atranorin showed potential due to its dual therapeutic action, its performance in stability and interaction analyses was less compelling compared to Sphenostylisin I and DMDBC, emphasizing the latter pair's superior promise for further development.

CONCLUSION

In this study, the potential of Sphenostylisin I and DMDBC as GKAs was thoroughly assessed through molecular docking, molecular dynamics simulations, ADME analysis, and binding-free energy calculations. Both compounds showed favorable binding affinities and excellent stability during MD simulations, along with strong binding free energy values, indicating their potential to activate glucokinase effectively. Despite slightly higher binding energies compared to the reference compound Piragliatin, their lack of liver-toxic functional groups sets them apart as promising candidates for drug development. The comparison with other compounds, including Camptothecin and Atranorin, further highlighted the unique stability and favorable properties of Sphenostylisin I and DMDBC, making them suitable alternatives to Piragliatin. Even though an extensive research was undertaken, in silico methods were relied on, presenting a limitation of the study.

Future research should focus on in vitro and in vivo testing of Sphenostylisin I and DMDBC to validate their glucokinase activation potential and assess their safety profile in biological systems. This should include exploring the metabolic pathways and toxicity of these compounds to ensure their suitability as long-term treatments for conditions like type 2 diabetes, while also considering potential interactions with other drugs. Further optimization of these compounds, combining in silico and lab assay, could also be considered to enhance their bioavailability and pharmacokinetic properties.

ACKNOWLEDGMENT

The authors acknowledge the Faculty of Pharmacy, Universitas Indonesia, for providing resources and the National Research and Innovation Agency of Indonesia (BRIN) for facilitating access to their computational services through the BRIN MAHAMERU HPC.

FUNDING

This research was supported by Universitas Indonesia through the PUTI grant No. NKB 602/UN2.RST/HKP.05.00/2024.

AUTHORS CONTRIBUTIONS

Ezekiel Makambwa contributed to the hypothesis formulation, conceptualization, data compilation, processing, analysis, and writing of the original and review drafts. Masteria Yunovilsa Putra provided supervision. Adha Dastu Illahi contributed to the molecular dynamic study and draft review. Muhammad Adil Khan assisted with hypothesis formulation and draft review. Arry Yanuar contributed to conceptualization and supervision.

CONFLICT OF INTEREST

The authors declare that there is no conflict of interest.

REFERENCES

1. Onikanni SA, Lawal B, Munyembaraga V, Bakare OS, Taher M, Khotib J, *et al*. Profiling the antidiabetic potential of compounds identified from fractionated extracts of *Entada africana* toward glucokinase stimulation: Computational insight. Molecules. 2023;28(15):5752. doi: 10.3390/molecules28155752, PMID: 37570723
2. Dahlén AD, Dashi G, Maslov I, Attwood MM, Jonsson J, Trukhan V, *et al*. Trends in antidiabetic drug discovery: FDA approved drugs, new drugs in clinical trials and global sales. Front Pharmacol. 2022;12:807548. doi: 10.3389/fphar.2021.807548, PMID: 35126141
3. Usai R, Majoni S, Rwere F. Natural products for the treatment and management of diabetes mellitus in Zimbabwe-a review. Front Pharmacol. 2022;13:980819. doi: 10.3389/fphar.2022.980819, PMID: 36091798
4. Mutowo M, Gowda U, Mangwiro JC, Lorgelly P, Owen A, Renzaho A. Prevalence of diabetes in Zimbabwe: A systematic review with meta-analysis. Int J Public Health. 2015;60(1):1-11. doi: 10.1007/s00038-014-0626-y, PMID: 25432797
5. Edelman SV, Polonsky WH. Type 2 diabetes in the real world: The elusive nature of glycemic control. Diabetes Care. 2017;40(11):1425-32. doi: 10.2337/dc16-1974, PMID: 28801473
6. Louie JZ, Shiffman D, Rowland CM, Kenyon NS, Bernal-Mizrachi E, McPhaul MJ, *et al*. Predictors of lack of glycemic control in persons with type 2 diabetes. Clin Diabetes Endocrinol. 2024;10(1):2. doi: 10.1186/s40842-023-00160-7, PMID: 38267992
7. Thilagavathi R, Hosseini-Zare MS, Malini M, Selvam C. A comprehensive review on glucokinase activators: Promising agents for the treatment of type 2 diabetes. Chem Biol Drug Des. 2022;99(2):247-63. doi: 10.1111/cbdd.13979, PMID: 34714587
8. Ren Y, Li L, Wan L, Huang Y, Cao S. Glucokinase as an emerging anti-diabetes target and recent progress in the development of its agonists. J Enzyme Inhib Med Chem. 2022;37(1):606-15. doi: 10.1080/14756366.2021.2025362, PMID: 35067153
9. Sharma P, Singh S, Sharma N, Singla D, Guarve K, Grewal AS. Targeting human Glucokinase for the treatment of type 2 diabetes: An overview of allosteric Glucokinase activators. J Diabetes Metab Disord. 2022;21(1):1129-37. doi: 10.1007/s40200-022-01019-x, PMID: 35673438
10. Taha MO, Habash M, Khanfar MA. The use of docking-based comparative intermolecular contacts analysis to identify optimal docking conditions within glucokinase and to discover of new GK activators. J Comput Aided Mol Des. 2014;28(5):509-47. doi: 10.1007/s10822-014-9740-4, PMID: 24610240
11. Li P, Zhu D. Clinical investigation of glucokinase activators for the restoration of glucose homeostasis in diabetes. J Diabetes. 2024;16(5):e13544. doi: 10.1111/1753-0407.13544, PMID: 38664885
12. Yadav S, Bharti S, Mathur P. GlucoKinaseDB: A comprehensive, curated resource of glucokinase modulators for clinical and molecular research. Comput Biol Chem. 2023;103:107818. doi: 10.1016/j.compbiolchem.2023.107818, PMID: 36680885
13. Sharma S, Wadhwa K, Choudhary M, Budhwar V. Ethnopharmacological perspectives of Glucokinase activators in the treatment of diabetes mellitus. Nat Prod Res. 2022;36(11):2962-76. doi: 10.1080/14786419.2021.1931187, PMID: 34044681
14. Adasme MF, Linnemann KL, Bolz SN, Kaiser F, Salentin S, Haupt VJ, *et al*. PLIP 2021: Expanding the scope of the protein-ligand interaction profiler to DNA and RNA. Nucleic Acids Res. 2021;49(W1):W530-4. doi: 10.1093/nar/gkab294, PMID: 33950214
15. Pettersen EF, Goddard TD, Huang CC, Couch GS, Greenblatt DM, Meng EC, *et al*. UCSF Chimera--A visualization system for exploratory research and analysis. J Comput Chem. 2004;25(13):1605-12. doi: 10.1002/jcc.20084, PMID: 15264254
16. Petit P, Antoine M, Ferry G, Boutin JA, Lagarde A, Gluais L, *et al*. The active conformation of human Glucokinase is not altered by allosteric activators. Acta Crystallogr D Biol Crystallogr. 2011;67(Pt 11):929-35. doi: 10.1107/s0907444911036729, PMID: 22101819
17. Krivák R, Hoksza D. P2Rank: Machine learning based tool for rapid and accurate prediction of ligand binding sites from protein structure. J Cheminform. 2018;10(1):39. doi: 10.1186/s13321-018-0285-8
18. Ali A. Development of antidiabetic drugs from benzamide derivatives as Glucokinase activator: A computational approach. Saudi J Biol Sci. 2022;29(5):3313-25. doi: 10.1016/j.sjbs.2022.01.058, PMID: 35844378
19. Forli S, Huey R, Pique ME, Sanner MF, Goodsell DS, Olson AJ. Computational protein-ligand docking and virtual drug screening with the AutoDock suite. Nat Protoc. 2016;11(5):905-19. doi: 10.1038/nprot.2016.051, PMID: 27077332
20. Hill AD, Reilly PJ. Scoring functions for AutoDock. Methods Mol Biol. 2015;1273:467-74. doi: 10.1007/978-1-4939-2343-4_27, PMID: 25753725
21. Morris GM, Lim-Wilby M. Molecular docking. Methods Mol

Biol. 2008;443:365-82. doi: 10.1007/978-1-59745-177-2_19, PMID: 18446297
22. Kurian T. Molecular docking study of Epigallocatechin gallate on FLT3 in complex with gilteritinib for anticancer activity. Asian J Pharm Clin Res. 2024;7(1):5-7. doi: 10.22159/ajpcr.2024.v17i1.48733
23. Bell EW, Zhang Y. DockRMSD: An open-source tool for atom mapping and RMSD calculation of symmetric molecules through graph isomorphism. J Cheminform. 2019;11(1):40. doi: 10.1186/s13321-019-0362-7
24. Daina A, Michielin O, Zoete V. SwissADME: A free web tool to evaluate pharmacokinetics, drug-likeness and medicinal chemistry friendliness of small molecules. Sci Rep. 2017;7(1):42717. doi: 10.1038/srep42717, PMID: 28256516
25. Michiba K, Watanabe K, Imaoka T, Nakai D. Recent advances in the gastrointestinal complex *in vitro* Model for ADME studies. Pharmaceutics. 2023;16(1):37. doi: 10.3390/pharmaceutics16010037, PMID: 38258048
26. Mora Lagares L, Minovski N, Novič M. Multiclass classifier for P-glycoprotein substrates, inhibitors, and non-active compounds. Molecules. 2019;24(10):2006. doi: 10.3390/molecules24102006, PMID: 31130601
27. Hakkola J, Hukkanen J, Turpeinen M, Pelkonen O. Inhibition and induction of CYP enzymes in humans: An update. Arch Toxicol. 2020;94(11):3671-722. doi: 10.1007/s00204-020-02936-7, PMID: 33111191
28. Pinal R. Enhancing the bioavailability of poorly soluble drugs. Pharmaceutics. 2024;16(6):758. doi: 10.3390/pharmaceutics16060758, PMID: 38931880
29. Tsopelas F, Giaginis C, Tsantili-Kakoulidou A. Lipophilicity and biomimetic properties to support drug discovery. Expert Opin Drug Discov. 2017;12(9):885-96. doi: 10.1080/17460441.2017.1344210, PMID: 28644732
30. Lemkul JA. Introductory tutorials for simulating protein dynamics with GROMACS. J Phys Chem B. 2024;128(39):9418-35. doi: 10.1021/acs.jpcb.4c04901, PMID: 39305267
31. Jo S, Kim T, Iyer VG, Im W. CHARMM-GUI: A web-based graphical user interface for CHARMM. J Comput Chem. 2008;29(11):1859-65. doi: 10.1002/jcc.20945, PMID: 18351591
32. Lee J, Cheng X, Swails JM, Yeom MS, Eastman PK, Lemkul JA, *et al*. CHARMM-GUI input generator for NAMD, GROMACS, AMBER, OpenMM, and CHARMM/OpenMM simulations using the CHARMM36 additive force field. J Chem Theory Comput. 2016;12(1):405-13. doi: 10.1021/acs.jctc.5b00935
33. Miller BR 3rd, McGee TD, Swails JM, Homeyer N, Gohlke H, Roitberg AE. MMPBSA.py: An efficient program for end-state free energy calculations. J Chem Theory Comput. 2012;8(9):3314-21. doi: 10.1021/ct300418h, PMID: 26605738
34. Valdés-Tresanco MS, Valdés-Tresanco ME, Valiente PA, Moreno E. gmx_MMPBSA: A new tool to perform end-state free energy calculations with GROMACS. J Chem Theory Comput. 2021;17(10):6281-91. doi: 10.1021/acs.jctc.1c00645, PMID: 34586825
35. Khamlich J, Douiyeh I, Saih A, Moussamih S, Regragui A, Kettani A, *et al*. Identification of small molecule Glucokinase activators for the treatment of diabetes based on plants from the traditional Chinese medicine: *In silico* analysis. Microb Pathog. 2024;195:106851. doi: 10.1016/j.micpath.2024.106851, PMID: 39197693
36. Min Q, Cai X, Sun W, Gao F, Li Z, Zhang Q, *et al*. Identification of mangiferin as a potential Glucokinase activator by structure-based virtual ligand screening. Sci Rep. 2017;7(1):44681. doi: 10.1038/srep44681, PMID: 28317897
37. Zhi J, Zhai S. Effects of piragliatin, a Glucokinase activator, on fasting and postprandial plasma glucose in patients with type 2 diabetes mellitus. J Clin Pharmacol. 2016;56(2):231-8. doi: 10.1002/jcph.589, PMID: 26183686
38. Anderson A. Final Report on the safety assessment of benzaldehyde. Int J Toxicol. 2006;25(Suppl 1):11-27. doi: 10.1080/10915810600716612, PMID: 16835129
39. Melo MG, dos Santos JP, Serafini MR, Caregnato FF, de Bittencourt Pasquali MA, Rabelo TK, *et al*. Redox properties and cytoprotective actions of atranorin, a lichen secondary metabolite. Toxicol *In Vitro*. 2011;25(2):462-8. doi: 10.1016/j.tiv.2010.11.014, PMID: 21111802
40. Kamle M, Pandhi S, Mishra S, Barua S, Kurian A, Mahato DK, *et al*. Camptothecin and its derivatives: Advancements, mechanisms and clinical potential in cancer therapy. Med Oncol. 2024;41(11):263. doi: 10.1007/s12032-024-02527-x, PMID: 39382779
41. Hegab MI. A review on chemical and biological studies of 4-chromanone derivatives. Russ J Organ Chem. 2023;59(3):483-97. doi: 10.1134/S107042802303017X
42. Park JE, Han JS. HM-chromanone suppresses hepatic glucose production via activation of AMP-activated protein kinase in HepG2 cell. Eur J Pharmacol. 2022;928:175108. doi: 10.1016/j.ejphar.2022.175108, PMID: 35718128
43. Cheng JL, He XR, Wang ZC, Zhang JG, Zhao JH, Zhu GN. Metabolism-based synthesis, biological evaluation and structure-activity relationship analysis of spirotetramat analogues as potential lipid biosynthesis inhibitors. Pest Manag Sci. 2013;69(10):1121-30. doi: 10.1002/ps.3473, PMID: 23436572
44. Li J, Pan L, Deng Y, Muñoz-Acuña U, Yuan C, Lai H, *et al*. Sphenostylisins A-K: Bioactive modified isoflavonoid constituents of the root bark of *Sphenostylis marginata* ssp. Erecta. J Org Chem. 2013;78(20):10166-77. doi: 10.1021/jo401573h
45. Li X, Wang D, Xia MY, Wang ZH, Wang WN, Cui Z. Cytotoxic prenylated flavonoids from the stem bark of *Maackia amurensis*. Chem Pharm Bull (Tokyo). 2009;57(3):302-6. doi: 10.1248/cpb.57.302, PMID: 19252325
46. Nahir CF, Putra MY, Wibowo JT, Lee VS, Yanuar A. The potential of Indonesian marine natural product with dual targeting activity through SARS-COV-2 3CLPRO and PLPRO: An *in silico* studies. Int J Appl Pharm. 2023;15(5):171-80. doi: 10.22159/ijap.2023v15i5.48416
47. Damghani T, Sedghamiz T, Sharifi S, Pirhadi S. Critical c-Met-inhibitor interactions resolved from molecular dynamics simulations of different c-Met complexes. J Mol Struct. 2020;1203:127456. doi: 10.1016/j.molstruc.2019.127456
48. Lobanov MY, Bogatyreva NS, Galzitskaya OV. Radius of gyration as an indicator of protein structure compactness. Mol Biol. 2008;42(4):623-8. doi: 10.1134/S0026893308040195
49. Al-Khafaji K, Taskin Tok T. Molecular dynamics simulation, free energy landscape and binding free energy computations in exploration the anti-invasive activity of amygdalin against metastasis. Comput Methods Programs Biomed. 2020;195:105660. doi: 10.1016/j.cmpb.2020.105660, PMID: 32726718
50. Wang C, Greene D, Xiao L, Qi R, Luo R. Recent developments and applications of the MMPBSA method. Front Mol Biosci. 2018;4:87. doi: 10.3389/fmolb.2017.00087, PMID: 29367919
51. Sahakyan H. Improving virtual screening results with MM/GBSA and MM/PBSA rescoring. J Comput Aided Mol Des. 2021;35(6):731-6. doi: 10.1007/s10822-021-00389-3, PMID: 33983518